Investigation of structural and magnetic properties of $PrIr_3B_2$ single crystal

Cite as: AIP Advances **9**, 035021 (2019); https://doi.org/10.1063/1.5079847
Submitted: 04 November 2018 • Accepted: 08 January 2019 • Published Online: 15 March 2019

S. Manni, A. Thamizhavel and S. K. Dhar

Investigation of structural and magnetic properties of $PrIr_3B_2$ single crystal

Cite as: AIP Advances 9, 035021 (2019); doi: 10.1063/1.5079847
Presented: 15 January 2019 • Submitted: 4 November 2018 •
Accepted: 8 January 2019 • Published Online: 15 March 2019

S. Manni,[1,2] A. Thamizhavel,[1] and S. K. Dhar[1,a)]

AFFILIATIONS

[1] Department of Condensed Matter Physics and Materials Science, Tata Institute of Fundamental Research, Homi Bhabha Road, Colaba, Mumbai 400 005, India
[2] Department of Physics, Indian Institute of Technology, Palakkad, Kerala 678 557, India

Note: This paper was presented at the 2019 Joint MMM-Intermag Conference.
[a)] **Electronic mail:** sudesh@tifr.res.in

ABSTRACT

We report the growth of a single crystal of $PrIr_3B_2$ by Czochralski pulling method and its structural and anisotropic magnetic properties. At room temperature, $PrIr_3B_2$ crystallizes in the hexagonal $CeCo_3B_2$-type ($P6/mmm$) structure. However, a change of crystal symmetry is indicated by a hysteretic transition observed in both the resistivity and heat capacity taking place at ≈ 280 K, which is similar to the observed transition from monoclinic (at room temperature) to hexagonal at 395 K previously reported in $CeIr_3B_2$ in literature. The jump in the heat capacity at the transition during cooling is nearly 400 J/mol K. The Curie-Weiss behavior of susceptibility conforms to a trivalent state of the Pr ions, which order antiferromagnetically or ferrimagnetically, as inferred from a relatively broad peak in the susceptibility centered around 10 K. The bulk magnetic transition is further corroborated by an anomaly in the heat capacity at low temperatures. Both the temperature dependence of magnetization, and the isothermal magnetization at 2 K reveal a highly anisotropic magnetic behavior in $PrIr_3B_2$ with c-axis [0001] as the hard direction of magnetization. The electrical resistivity shows normal metallic behavior down to T_N, below which it shows an upturn suggesting the onset of superzone gap.

The compounds of RT_3B_2 (R = Ce and Pr; T = Rh and Ir) show interesting magnetic and structural properties. $CeRh_3B_2$, crystallizing in the hexagonal $CeCo_3B_2$-type structure ($P6/mmm$), is a ferromagnet with the highest Curie temperature T_C of ≃120 K for any compound of Ce with other non-magnetic elements.[1] $PrRh_3B_2$ is iso-structural to $CeRh_3B_2$ and it orders ferrimagnetically at ≃3.6 K with an Ising triangle spin structure.[2] The large anisotropic magnetization of $PrRh_3B_2$ was well explained as arising due to a large overall crystal electric field (CEF) splitting energy of 1080 K. RIr_3B_2 (R = Ce, Nd-Lu; Sc and Y) were initially reported to adopt a base-centered monoclinic structure with the possible space group $C2/m$ and two formula units per unit cell.[3] There was no information on the crystal structure of $PrIr_3B_2$ in Ref. 3. Using x-ray powder and single crystal diffraction, Sologub et al. in a later work inferred the hexagonal, $CeCo_3B_2$-type structure for $CeIr_3B_2$ and $PrIr_3B_2$.[4] Working on a single crystal of $CeIr_3B_2$ grown by Czochralski pulling method, Kubota *et al.* found that there is a structural transition from room temperature monoclinic to hexagonal symmetry approximately at 395 K on heating.[5] Somewhat similar to its Rh-analog, $CeIr_3B_2$ orders ferromagnetically with a relatively high T_C of 41 K. The ferromagnetic saturation moment at 1.8 K was found to be 0.04 μ_B/Ce, which is almost an order of magnitude lower than the corresponding figure in $CeRh_3B_2$. In view of the observed magnetic and structural properties and the presence of strong CEF in these compounds, we have undertaken a study of single crystalline $PrIr_3B_2$ and the results are reported here.

A single crystal of $PrIr_3B_2$ was grown by Czochralski pulling method in a tetra arc furnace under an inert atmosphere of argon. Initially, a polycrystalline ingot weighing nearly 10 g was melted, flipping over the as-cast button several times to ensure homogeneity. A piece of $PrIr_3B_2$ polycrystal was used as seed and momentarily dipped into the melt and the crystal was pulled at a speed of 10 mm/h. $LaIr_3B_2$ poly-crystal was synthesized by arc-melting the high purity metals in stoichiometric composition. Laue diffraction

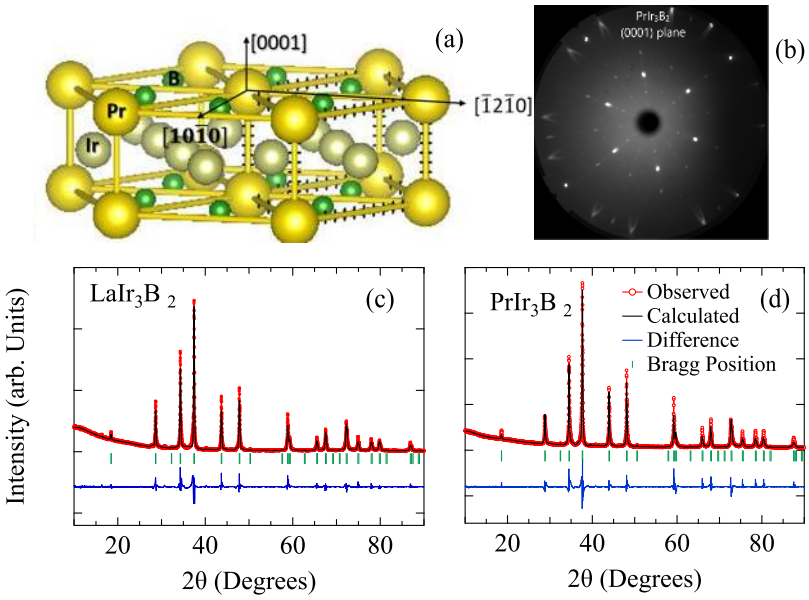

FIG. 1. (a) Hexagonal crystal structure of $PrIr_3B_2$ at room temperature. (b) Laue diffraction pattern of the $PrIr_3B_2$ single crystal oriented along [0001] direction. Rietveld refinement of powder XRD data of (c) $LaIr_3B_2$ poly-crystal and (d) crushed single crystal of $PrIr_3B_2$ with *P6/mmm* crystal structure.

method was used to characterize the symmetry of the single crystal and to orient it along the desired directions, at room temperature and powder x-ray diffraction (Cu-K_α radiation of λ = 1.5418 Å) was used to find the lattice parameters at 300 K. MPMS and PPMS (Quantum Design, USA) were used to measure the magnetization (1.8 to 300 K; 0 to 7 T), and the heat capacity and electrical resistivity (1.9 to 340 K), respectively.

The Laue diffraction pattern taken on a piece cut from the nearly 5 cm long specimen pulled from the melt showed sharp diffraction spots characteristic of hexagonal symmetry. Figure 1(b) shows Laue diffraction for the crystal piece oriented along [0001] direction. The crystal was then cut along the principal crystallographic directions along *viz.*, [10$\bar{1}$0], [$\bar{1}$2$\bar{1}$0] and [0001] for electrical, magnetic and heat capacity measurements. The hexagonal crystal structure is shown in Fig. 1(a). Powder x-ray diffraction patterns obtained by crushing a small portion of the $LaIr_3B_2$ polycrystal [Fig. 1(c)] and $PrIr_3B_2$ single crystal [Fig. 1(d)] could be neatly refined on the basis of hexagonal, *P6/mmm*, symmetry with lattice parameters $a = b$ = 5.546 Å, c = 3.1145 Å and $a = b$ = 5.5149 Å, c = 3.0957 Å, respectively, by Rietveld method using Fullprof software.[6] The Bragg R-values of the fit are 7.51 and 5.92, respectively. The absence of any spurious peaks confirmed the phase purity of our single crystal and poly-crystal. In view of the symmetry change reported in $CeIr_3B_2$, and our data on the electrical resistivity and heat capacity of $PrIr_3B_2$ (see below), we infer a structural transiton just below room temperature.

A single crystal enables us to explore the anisotropic behavior of various physical properties, like magnetization and electrical resistivity in the present case, when the external agents such as magnetic field or electrical current density are applied along particular directions of the unit cell. In the present case the alignment of the specimen along the crystallographic directions was done at room temperature where the crystal exists in the hexagonal symmetry. Therefore, the directions of the applied field and the current density below the structural transition are only notional with respect to the hexagonal unit cell. It has been pointed out earlier that the monoclinic structure can be viewed as a slightly distorted hexagonal $CeCo_3B_2$-type.[3] In particular the c-axes coincide in both the structure types.

The inverse magnetic susceptibility between 1.8 and 300 K is shown in Fig. 2. While the response is nearly isotropic in the *ab*-plane, there is a large anisotropy in the susceptibility between the

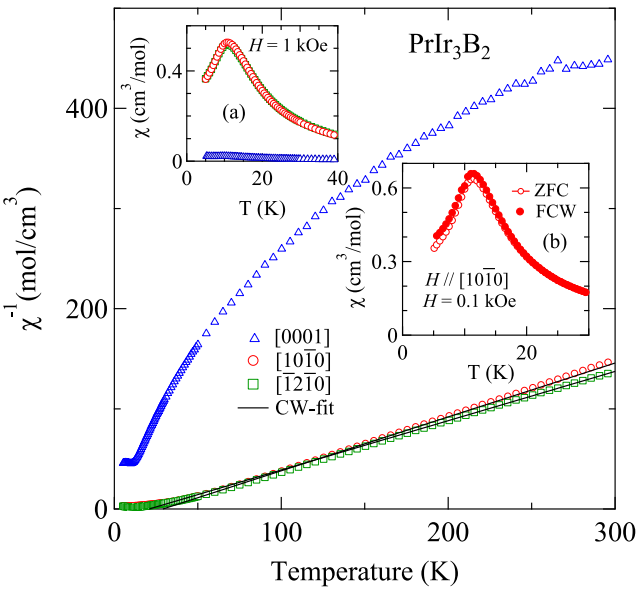

FIG. 2. Inverse magnetic susceptibility ($1/\chi$) of $PrIr_3B_2$ single crystal for field along three principal crystallographic directions. Inset (a): χ *vs* T, zoomed at low temperature. Inset (b): Field cooled (FCW) and ZFC susceptibility measured for H || [10$\bar{1}$0], at a field H = 0.1 kOe.

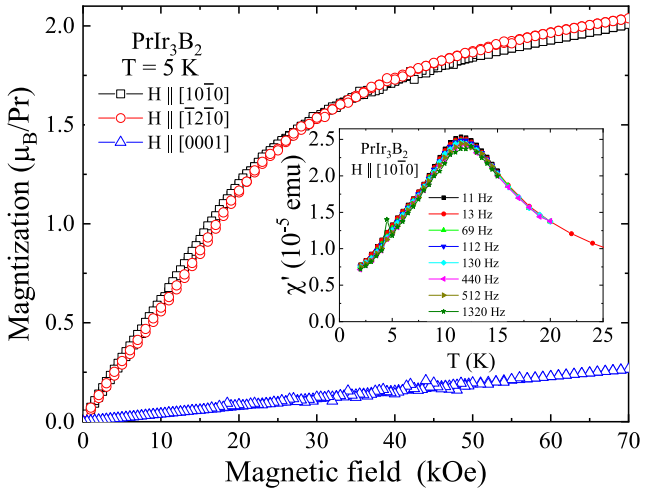

FIG. 3. Isothermal magnetization (*M vs H*) measured on $PrIr_3B_2$ single crystal for field along three principal crystallographic directions at T = 5 K. Inset shows temperature dependent ac susceptibility (χ') at different frequencies.

ab-plane and *c*-axis. The data in the *ab*-plane could be fitted to the Curie-Weiss law with μ_{eff} = 3.83 and 4.0 μ_B/Pr. and θ_p = 29.7 and 24.4 K for $H \parallel [10\bar{1}0]$ and $[\bar{1}2\bar{1}0]$, respectively. The μ_{eff} values somewhat exceed the value of 3.58 μ_B for Pr^{3+} and positive θ_p indicates a predominant ferromagnetic interaction in the *ab*-plane. χ^{-1} shows an appreciable curvature along the *c*-axis and a fit to Curie-Weiss law does not appear feasible. It may be noted that the susceptibility data do not exhibit any distinguishable anomaly at the structural transition. The low temperature susceptibility below 40 K is shown in the inset (a) of Fig. 2. Susceptibility shows a peak near 10 K for fields applied in the *ab*-plane indicating the transition to an antiferromagnetic state. For $H \parallel c$-axis the susceptibility is nearly independent of temperature below T_N and relatively more than an order of magnitude smaller. The right inset of Fig. 2 shows the susceptibility measured in ZFC (zero-field-cooled) and FCW (field-cooled-warming) mode for $H \parallel [10\bar{1}0]$ in the neighborhood of T_N. The near coincidence of the two susceptibilities below T_N, at low field (H = 0.1 kOe) is in conformity with the antiferromagnetic nature of the magnetic transition. To explore further the very slight bifurcation between ZFC and FCW data, we have measured the ac susceptibility, χ' at selected frequencies from 11 to 1320 Hz between 2 and 20 K. The data are plotted in Fig. 3 inset. χ' shows a broad peak around 10 K with no discernible frequency dependence ruling out any spin glass freezing of Pr-moments.

The results of isothermal magnetization at 5 K are in full correspondence with the susceptibility data presented above. The magnetization for $H \parallel [0001]$ varies linearly with field right up to the highest field of 70 kOe attaining a value of just 0.25 μ_B/Pr, as shown in Fig. 3. On the other hand, in the *ab*-plane the magnetization is again isotropic for the two directions attaining a value of 2 μ_B/Pr at 70 kOe, which is almost an order of magnitude higher than the corresponding value along the *c*-axis. For the field applied along two directions in the *ab*-plane, in dM/dH there is a shallow peak around 15 kOe (not shown here), suggesting a possible spin-flop transition. These data suggest that *ab*-plane is the easy-plane and the *c*-axis the hard axis of magnetization. Since a zero magnetization is not seen at fields below the spin-flop, it indicates a relatively more complex configuration of the Pr-moments in the antiferromagnetic state compared to the simple bipartite collinear antiferoomagnet.

The heat capacity of $PrIr_3B_2$ and the non-magnetic reference $LaIr_3B_2$ between 1.9 and 300 K are plotted in the main panel of Fig. 4 (a). For Pr-analog, data taken in both cooling and heating cycles near room temperature are shown in the bottom inset. A huge anomaly with hysteresis is seen in the range 275-285 K. The jump in the heat capacity at the transition during cooling is nearly 400 J/mol K. The hysteretic anomaly in the heat capacity indicates a structural transition and maybe a change of crystal symmetry as observed in $CeIr_3B_2$.[5] The heat capacity data below 20 K are depicted in the top inset of Fig. 4 (a). A mild anomaly is observed at the magnetic transition, which is relatively muted compared to the robust lambda type anomalies characteristic of long-range magnetic order. Assuming the phonon spectra of Pr and La compounds are identical, the $4f$-derived heat capacity C_{4f}, and the entropy, S_{4f}, are plotted in the left-axis of Fig. 4 (b). S_{4f} is calculated by integrating C_{4f}/T. The peak at the transition looks relatively sharper after the phonon contribution is subtracted; the entropy $R\ ln2$ associated with an effective spin-half doublet ground state is released by about 20 K.

The electrical resistance measured in the temperature range 1.8 to 340 K of $PrIr_3B_2$ is shown in Fig. 5 as normalised resistance $R(T)/R(340\ K)$ *vs.* T. The data show a hysteretic transition between 250 and 280 K (refer to the inset of Fig. 5), providing additional evidence for the structural transition inferred above from heat capacity. A two-step feature is observed in *Norm. Resitance vs T*, near the structural transition. It needs to be investigated further to understand its origin. Below the structural transition the resistivity

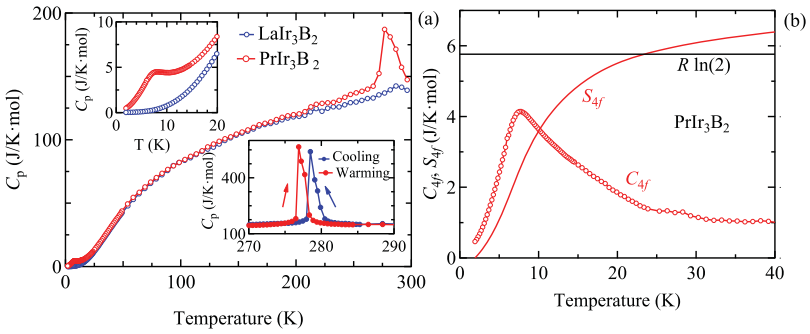

FIG. 4. (a) Heat Capacity (C_p) *vs.* Temperature (T) of $PrIr_3B_2$ single crystal and $LaIr_3B_2$ polycrystal at zero field. Top inset of (a) C_p *vs.* T at low temperature near T_N, bottom inset of (a) C_p *vs.* T of $PrIr_3B_2$ single crystal near structural transition during cooling and heating. (b) $4f$-contribution of heat capacity (C_{4f}) and entropy S_{4f} *vs.*T for $PrIr_3B_2$.

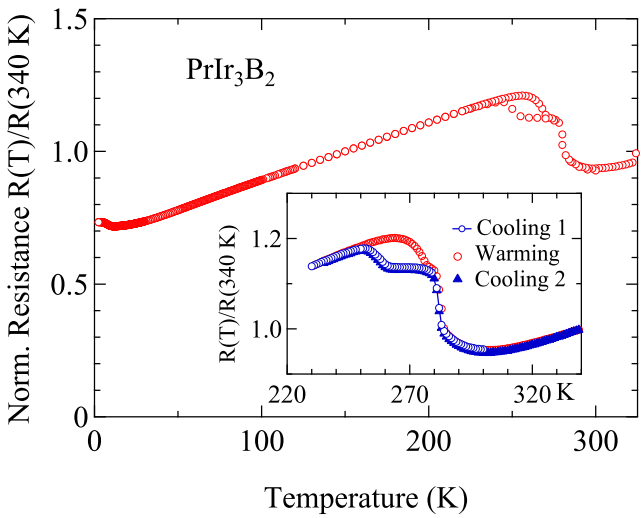

FIG. 5. Normalised resistance *vs.* *T* of $PrIr_3B_2$ single crystal at zero field for current, $J \parallel [10\bar{1}0]$. Inset shows *R vs T* data during 1st cooling, 1st heating and 2nd cooling near the structural transition.

shows a metallic behavior decreasing with temperature. It shows an upturn at the magnetic transition which is tentatively attributed to the superzone-gap induced by the antiferromagnetic ordering of the Pr-moments.

In conclusion, we have synthesized high quality single crystal of $PrIr_3B_2$ and investigated its structural, electrical, magnetic and thermodynamic properties. We propose a structural transition near T_s = 280 K inferred from hysteretic heat capacity and electrical transport in the vicinity of T_s and a huge jump in the heat capacity across T_s. Magnetic ordering is confirmed from magnetic, transport and thermodynamic measurements. An anomaly near 10 K confirms the antiferromagnetic transition at low temperature, where a super-zone gap opens at fermi surface. The anomaly in heat capacity at T_N is broad; it may be due to low-lying CEF levels, or due to peculiarity in the low temperature crystal structure which at present is not known.

REFERENCES

[1] S. K. Dhar, S. K. Malik, and R. Vijayaraghavan, J. Phys. C (Solid State Phys.) **14**, L321 (1981).
[2] M. Yamada, Y. Obiraki, T. Okubo, T. Shiromoto, K. Yu, M. Shiimoto, H. Kohara, T. Yamamoto, D. Honda, A. Galatanu, Y. Haga, T. Takeuchi, K. Sugiyama, R. Settai, K. Kindo, S. K. Dhar, H. Harima, and Y. Ōnuki, J. Phys. Soc. Jpn. **73**, 2266 (2004).
[3] H. C. Ku and G. P. Meisnner, J. Less Common Metals **78**, 99 (1981).
[4] O. Sologub, C. Rizzoli, P. Salamakha, and H. Isper, J. Alloys Compd. **360**, 127 (2003).
[5] K. Kubota, E. Matsuoka, Y. Funasako, T. Mochida, T. Sakurai, H. Ohta, T. Onimaru, T. Takabatake, and J. Hitoshi Sugawara, Phys. Soc. Jpn. **82**, 104715 (2013).
[6] J. Rodriguez-Carvajal, Physica B **192**, 55 (1993).